Contribution Analysis of Uncertainty Parameters in MAAP5 Dynamic Event Tree Simulation of Station Blackout

Ikuo Kinoshita[a]
[a] Institute of Nuclear Safety System, Inc., 64 Sata, Mihama, Mikata, Fukui, Japan,
kinoshita@inss.co.jp

Abstract: Dynamic event tree (DET) analysis integrates thermal-hydraulic system models with safety system and operator response models and is widely used for dynamic risk quantification in nuclear power plants. While DET frameworks represent aleatory uncertainties using branching methods such as ADAPT, severe accident system codes employed in DET analyses contain significant epistemic uncertainties associated with physical modeling of severe accident phenomena. Therefore, a systematic framework to evaluate the impact of epistemic uncertainties on risk metrics is essential. As a first step toward this objective, this study presents a parameter contribution analysis for a station blackout scenario in a pressurized water reactor plant. The Zion nuclear power plant model implemented in the MAAP5 severe accident code was adopted. Important physical phenomena during station blackout were categorized into thermal-hydraulics, core pre-damage, core post-damage, and lower head behavior. Thirty-one physical model parameters associated with these phenomena were selected as epistemic uncertainty parameters. A total of 93 MAAP5 simulations were performed, and parameter importance was evaluated with respect to reactor vessel failure timing using SHAP-based contribution analysis. The results identified the maximum shear stress of the penetration tube, the heat sink heat transfer scale factor, lower head debris pool convective heat transfer, and collapse node porosity as dominant parameters influencing vessel failure progression. The analysis further indicated that complex interactions between the accumulator system and the primary system during intermittent passive injection significantly affect the distribution of core damage progression, while having limited influence on reactor vessel failure probability. These findings suggest that explainable machine learning–based contribution analysis provides a useful tool for interpreting epistemic uncertainty effects in dynamic event tree–based severe accident risk assessments. The proposed framework contributes to enhancing transparency and interpretability in uncertainty propagation within dynamic probabilistic risk assessment.

1. INTRODUCTION

Nuclear power plants (NPPs) frequently undergo modifications—such as equipment replacement, performance upgrades, and safety enhancements—to extend their operational life or to improve economic performance through power uprates and increased fuel burnup. Since these modifications can alter safety characteristics during transient or accident conditions, it is essential to quantitatively evaluate potential risk increases, such as core damage frequency, and ensure that sufficient safety margins are maintained.

A fundamental requirement for evaluating safety margins is the characterization of uncertainties associated with risk estimation. In typical NPP accident scenarios, complex dynamic interactions occur between physical processes and safety system responses. Therefore, quantifying uncertainties in both physical and probabilistic response model parameters is crucial.

One promising approach is the dynamic event tree (DET) method coupled with NPP simulation models [1-2]. This framework generates event sequences through integrated accident simulations, calculating risk based on sequence outcomes and initiating event probabilities. This integrated modeling enables a rational estimation of risk structure changes due to plant modifications, while sensitivity analysis allows for the prioritization of such updates.

Furthermore, the DET method facilitates the propagation of physical model uncertainties. In conventional probabilistic safety assessment (PSA), these uncertainties are typically addressed through conservative assumptions. However, uncertainties in severe accident codes are substantial and can significantly influence the overall risk structure. In contrast, the DET approach offers a more realistic assessment by incorporating epistemic uncertainties of physical model parameters alongside other epistemic and aleatory parameters. This enables the evaluation of simulation code refinement priorities through sensitivity analysis.

As a precedent, Rahman et al. [3] utilized the TRACE code (V5.0 P03) to quantify uncertainties in physical and probabilistic response models during a station blackout (SBO) scenario at the Zion plant; they evaluated the impact of the uncertainties on core damage frequency using Pearson and Spearman correlation coefficients.

In this study, an analysis of the same SBO scenario is performed using the severe accident analysis code MAAP5 [4]. Focusing on the progression from core damage to reactor pressure vessel (RPV) failure, key phenomena are identified and the impact of physical model uncertainties in MAAP5 on vessel failure frequency is evaluated using SHAP value analysis [5].

2. DESCRIPTION OF SBO ACCIDENT SEQUENCE AND RISK MODEL

SBO accidents are often a dominant contributor to the core damage frequency of nuclear power plants. An SBO is defined as the loss of off-site power concurrent with the failure of on-site emergency diesel generators, resulting in the loss of core cooling capability, including the emergency core cooling system (ECCS). In such scenarios, the turbine-driven auxiliary feedwater system (AFWS) is typically activated to maintain core cooling via secondary-side heat removal. If the AFWS is unavailable, the restoration of AC power becomes essential to initiate feed and bleed (FB) operations for core damage prevention. During FB operations, operators depressurize the primary system using the pressurizer (PZR) power-operated relief valves (PORVs) to allow coolant injection via the safety injection systems. Consequently, the timing of power restoration and the efficacy of operator response during FB operations are critical factors governing the progression and outcome of SBO accident scenarios.

2.1. Reference Accident Sequence

This study examines an SBO sequence involving the loss of AFWS followed by a failure of power restoration for FB operations. This sequence was derived by screening and modifying the loss of offsite power (LOSP) PSA event tree described in [6], and it was subsequently reviewed by the OECD/NEA CSNI Task Group SM2A [7]. The sequence is illustrated in Fig. 1.

Reference Sequence 12 initiates with a transient triggered by a turbine trip resulting from an LOSP. In response to the turbine trip, a reactor scram is automatically initiated. Emergency power sources (e.g., diesel generators) are required to support all essential safety loads; however, in this sequence, the emergency diesel generators fail to start upon demand. Under normal conditions, the turbine-driven auxiliary feedwater (AFW) pumps would be activated as the main feedwater pumps become unavailable. In this specific sequence, however, the AFW pumps also fail to operate, leading to the station blackout (SBO) scenario accompanied by a loss of AFW and hereafter called the TMLB' scenario. Following a loss-of-coolant accident (LOCA) condition caused by pump seal failure, core cooling must be maintained through the FB process. For the FB top event, operators are required to manually open the PZR PORVs to establish a bleed path and ensure coolant injection by starting at least one high-pressure safety injection pump. Therefore, a successful FB operation requires both the operator's action to secure the bleed path and the restoration of AC power to drive the safety injection pumps before core uncovery occurs. The cue for the operator's bleed action is provided by the low water level in the steam generators (SGs) resulting from inventory loss through automatic SG relief. In the current analysis, a 20-minute delay in operator response is assumed. Subsequently, the depressurization of the primary system via the

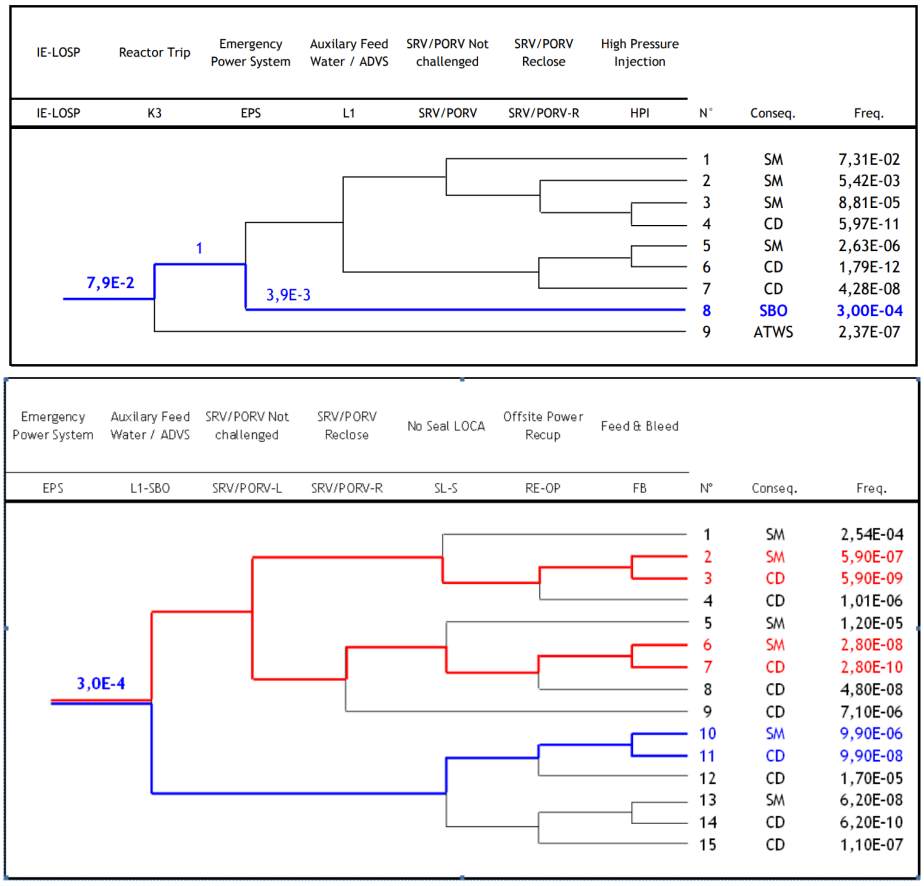

Figure 1: Loss of offsite power event tree (top); SBO accident sequence event tree (bottom) [6-7]

bleed operation allows for coolant injection from the accumulators, which are assumed to be available. Reference Sequence 12 considers the case where power restoration fails, ultimately leading to core damage due to the lack of safety injection.

2.2. Risk Model

The initial event frequency of the SBO and the failure probability for each heading related to the TMLB' transient are listed in Table 1.

In the analyzed TMLB' sequence, safety injection (or electrical power recovery) is not explicitly considered. It is known that an early recovery avoids core damage, whereas a late recovery leads to core damage. These recovery times may vary from a few minutes to several hours. Fouet et al. [8] proposed to use an exponential law to calculate the failure probability of power recovery (P_{FPR}) as

$$P_{FPR}(t) = exp\left(\frac{-t}{\tau}\right) \quad (1)$$

where, t represents the delay in power restoration (in hours), and τ is the mean value (assumed to be 1 hour in this study). Core damage can be prevented by safety injection if power is restored within a few minutes (defined as 10 minutes in [8]) before the peak cladding temperature (PCT) reaches 1473 K. This latest time t for power restoration required to prevent core damage is used to determine the probability of power restoration failure in Equation (1). Subsequently, the core damage frequency of the reference sequence is evaluated by considering both the failure probability of power recovery and the SBO frequency.

Table 1: Initial events and failure probabilities ([6-7])

Event	Description	Probability
IE-LOSP	Initial Event	7.9E-2
EPS	Emergency Power System	3.9E-3
L1-SBO	Auxiliary Feed water	8.9E-2
SL-S	Main Coolant Pump Seal LOCA	6.3E-3
RE-OP	Offsite Power Recovery	6.3E-1
FB	Feed and Bleed	1.0E-2

3. MAAP5 DYNAMIC EVENT TREE SIMULATIONS

In this study, the system code MAAP5 [4] was used for accident analysis. MAAP5 is an integrated plant response simulation code developed by the Electric Power Research Institute (EPRI) for the analysis of severe accidents in light water reactors.

3.1. Analysis Assumptions and Boundary Conditions

The main analysis assumptions and boundary conditions for the TMLB' scenario considered here are summarized in Table 2. The initial core power was set to 3250 MW, and the SG secondary-side water inventory was assumed to be 47.2 tons. The main steam relief valve was configured to open at 7.343 MPa. The pressurizer safety valve had a capacity of 15 cm^2, with opening and closing setpoints of 16.2 MPa and 15.7 MPa, respectively. The PZR PORV capacity was set to 45 cm^2, and it was assumed to open 25 minutes after the SG secondary-side water level decreased to 6.53 m or below. The accumulator injection was initiated at a pressure of 4.24 MPa, with a total water volume of 24.1 m^3.

Table 2: Analysis conditions

Device operation	Analysis conditions
Initial core power	3250 MW
SG secondary side water volume	47.2 tons
Main steam relief valve setpoint	Open: 7.343 MPa
PZR safety valve capacity	15 cm^2
PZR safety valve setpoints	Open: 16.2 MPa, Close: 15.7 MPa
PZR PORV capacity	45 cm^2
FB through PZR PORVs	When the SG secondary side water level is $\leq$ 6.53 m, the PZR PORV opens after a delay of 25 minutes.
Accumulators opening	Open: 4.24 MPa
Accumulators water volume	24.1 m^3

The event began with a reactor trip caused by a loss of feedwater. This triggered a reactor scram and subsequent trips of the reactor coolant pumps and main feedwater pumps. Since the feedwater supply had stopped, the water in the SGs evaporated as decay heat was transferred from the primary side to the secondary side. Within several seconds, the pressure in the SGs reached the setpoint (7.343 MPa) of the steam generator power-operated relief valves (SG PORVs). While the opening of the SG PORVs suppressed further pressure increase on the secondary side, SG water inventory was lost through the valves. When the SG secondary-side water level reached 6.53 m, the bleed path was opened by the operator's action. This action was assumed to have a 25-minute delay.

3.2. Dynamic Event Tree Analysis

The power recovery timings were set as follows.

- Base case: No power recovery
- Case1: t =13,000 s (Before core damage)
- Case2: t =15,000 s (After core damage, before debris relocation to the lower head)
- Case3: t =17,000 s (After core damage, before debris relocation to the lower head)
- Case4: t =19,000 s (After debris relocation to the lower head, before RV failure)

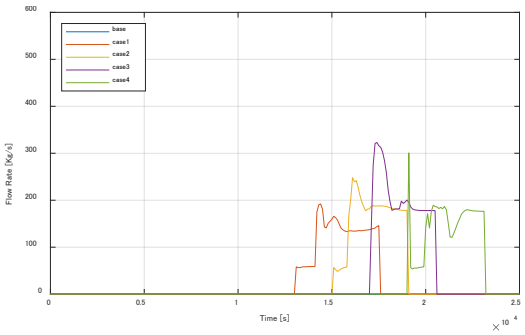

(a) SI flow rates

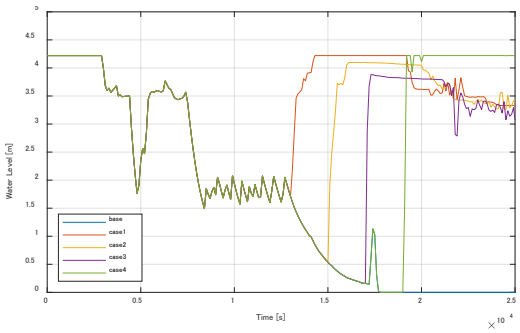

(b) Core water level

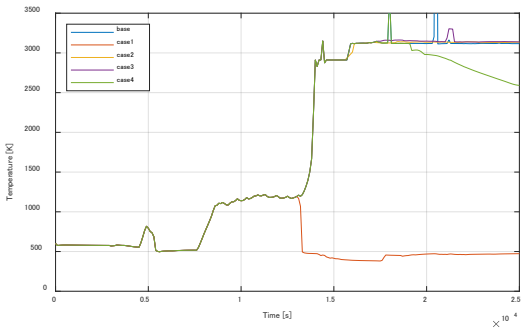

(c) Rod surface temperature

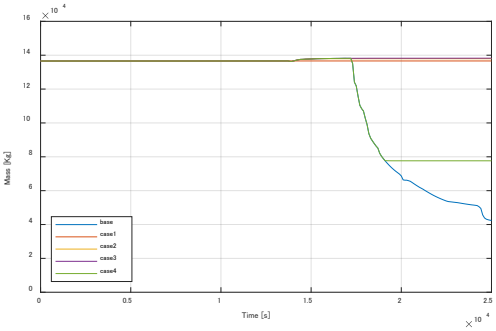

(d) Core debris mass

Figure 2: Dynamic event tree analysis results

Base case (No power recovery): When the accumulator tanks were depleted at approximately 12,600 s, the core water level began to decrease, and the PCT rose sharply (Fig. 2(c)). Since the core water level did not recover, the core could not be cooled, leading to core damage at approximately 13,968 s. Subsequently, at approximately 17,292 s, the core debris began relocating to the lower head, eventually resulting in reactor vessel (RV) failure.

Case 1 (Before core damage): By restoring external power before core damage occurred (13,000 s), the safety injection (SI) system was activated (Fig. 2(a)), and the core water level quickly recovered (Fig. 2(b)). The PCT also decreased promptly (Fig. 2(c)), and the sequence did not result in core damage.

Cases 2 and 3 (After core damage but before debris relocation to the lower head): By restoring external power after core damage but before debris relocates to the lower head (15,000 s and 17,000 s), the SI system was activated, and the core water level recovered rapidly (Fig. 2(b)). However, the PCT did not decrease and remained at a high temperature (Fig. 2(c)). The debris was maintained within the core, and relocation to the lower head did not occur (Fig. 2(d)).

Case 4 (After debris relocation to the lower head but before RV failure): By restoring external power after debris relocation to the lower head but before RV failure (19,000 s), the SI system was activated, and the core water level recovered quickly (Fig. 2(b)). A gradual downward trend in PCT was observed from 19,000 s (Fig. 2(c)). Unlike Cases 2 and 3, the debris within the core had decreased due to

relocation to the lower head; this reduction in core debris mass likely enhanced coolability, leading to the declining PCT trend. Due to the recovery of the core water level, the relocation of debris to the lower head ceased, and reactor vessel failure was averted.

4. UNCERTAINTY ANALYSIS

4.1. Uncertainty Parameters

The following literature was consulted to identify the important phenomena of the TMLB' scenario. Rahman et al. [3], cited for the accident sequence setting, summarized an analysis using the TRACE code (V5.0 P03) for a SBO scenario at the Zion plant that was aimed at quantifying uncertainties in physical models and probabilistic response model parameters. To extract key phenomena that could influence RV failure in the TMLB' scenario, the PIRT (phenomena identification and ranking table) analysis report [9] for severe accidents, conducted in response to the Fukushima Daiichi accident, was referenced. This report compiled investigation results intended to identify various phenomena during a severe accident and to select high-priority items to address challenges in simulating accident progression and source term evaluations. In a TMLB' scenario, if the operator's action to open the PZR PORVs is delayed, the primary system pressure may decrease due to hot leg failure caused by high-temperature core gases. In such a case, the primary system remains at high pressure at the time of RV failure, potentially leading to high-pressure melt ejection (HPME) and direct containment heating (DCH). Therefore, the ranking of key phenomena for HPME and DCH was also consulted from a publicly available document [10], which summarizes the applicability of the MAAP code for effectiveness evaluations of severe accident management measures.

The important phenomena of the TMLB' event were categorized into thermal-hydraulics, pre-core damage, post-core damage, and lower head behavior. By reviewing the MAAP5 code manuals, 31 physical model parameters related to these phenomena were selected as epistemic uncertainty parameters. The selected uncertainty parameters are listed in Table 3.

4.2. Evaluations of the Core Damage and Vessel Failure Frequency

In this study, an uncertainty analysis was performed for the Base case (without power restoration) described in Section 3.2. A total 93 parameter sets were randomly sampled from those shown in Table 3, and MAAP5 simulations were performed to evaluate the core damage frequency and RV failure frequency. According to the order statistics method [11], 95%/95% tolerance limits can be calculated from an analysis with this sample size.

Fig. 3(a) shows the time history of the PCT. The black line represents the Base case, while the gray lines represent the results of the uncertainty analysis. The red and green lines indicate the Base case and uncertainty analysis results by Rahman et al. [3], respectively. It was confirmed that these results generally fell within the range of the uncertainty analysis in this study. In the uncertainty analysis, all 93 sampled parameter sets resulted in RV failure; among these, the vast majority (88 sets) reached RV failure due to penetration tube ejection. Fig. 3(b) shows the time history of FEJPT which was the MAAP5 decision parameter related to penetration tube ejection. It was observed that FEJPT rose sharply starting from approximately 19,000 s, leading to RV failure.

Fig. 4(a) shows the cumulative distribution function (CDF) of the core damage time (the time when PCT exceeded 1,473 K). The core damage time ranges from 8,401 s to 14,201 s. As seen from the shape of the CDF, the distribution of core damage time was bimodal. As pointed out by Rahman et al. [3], this was considered to be due to uncertainties in cold leg condensation during accumulator injection. Fig. 4(b) shows the CDF of the reactor vessel failure time. The reactor vessel failure time ranged from 19,002 s to 21,805 s. The distribution of reactor vessel failure time was unimodal.

Table 3: Uncertainty parameters and their ranges

Important Phenomena	Parameters	Range	Distribution
Thermal-hydraulics			
Core boiling and changes in void Fraction	(1) FCHFCR [-]	[0.0036, 0.3]	Uniform
	(2) Nucleate boiling liquid-phase heat transfer coefficient multiplier [-]*	[0.5, 0.2]	Uniform
Gas-liquid separation and counter-current flow in the core	(3) FVOL [-]	[1.0, 2.5]	Uniform
	(4) Interfacial friction coefficient multiplier [-]*	[0.13, 3.0]	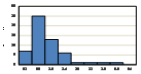
Heat transfer with structural materials of primary system	(5) FEQSIG [-]	[0.5, 2.0]	Uniform
	(6) FYLMP (2,1:2) [-]	[-0.05, 0.05]	Uniform
	(7) SCALH [-]	[0.5, 10.0]	Uniform
	(8) AGOBHL/AGOUHL [M^2]	[1.27e-4, 3.24e-2]	Uniform
Interfacial friction in the upper plenum, hot leg, and pressurizer	(9) Interfacial friction coefficient multiplier [-]*	[0.5, 2.0]	Uniform
Core pre-damage			
Decay heat	(10) QCR0 [-]	[0.95, 1.05]	Uniform
Zirconium–steam oxidation reaction	(11) FAOX [-]	[1.0, 2.0]	Uniform
	(12) Cladding tube oxidation coefficient multiplier [-]*	[0.54, 1.16]	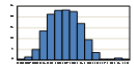
Fuel cladding ballooning	(13) Cladding tube deformation coefficient multiplier [-]*	[0.86, 1.07]	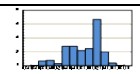
Fuel rod surface heat transfer	(14) Uncovered core heat transfer coefficient multiplier [-]*	[0.58, 1.88]	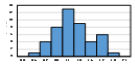
Core post-damage			
Molten fuel candling	(15) FVISC [-]	[0.1, 1000]	Uniform
Flow blockage caused by fuel rods debris	(16) EPSCU2 [-]	[0.001, 0.35]	Uniform
Flow blockage in the core and bypass regions caused by molten fuel	(17) EPSCUT [-]	[0.0, 0.25]	Uniform
Fuel rod degradation and relocation to the lower region	(18) TCLMAX [K]	[100, 3000]	Uniform
	(19) TSPFAL [K]	[1000, 3113]	Uniform
	(20) FDPOOL/FSPOOL/FUPOOL [-]	[0.01, 2.0]	Uniform
	(21) VFCRCO [-]	[0.05, 0.35]	Uniform
Lower head			
Corium–lower head heat transfer	(22) CDU [-]	[1.0, 3.0]	Uniform
	(23) CDCMLP [-]	[1.0, 100.0]	Uniform
	(24) Lower head debris pool convective heat transfer coefficient multiplier [-]*	[0.9, 1.1]	Uniform
Heat transfer between crust and water, Heat transfer between crust and the lower head	(25) XGAPLH [M]	[1.0e-6, 3.0e-4]	Uniform
	(26) XGAPTOPLH [M]	[1.0e-6, 2.0e-2]	Uniform
	(27) XXPSMN [M]	[0.0001, 0.0050]	Uniform
	(28) XXPSMU [M]	[0.01, 0.5]	Uniform
	(29) Gap cooling coefficient multiplier [-]*	[2.05, 2.32]	Uniform
Penetration tube melting	(30) ECREPP [-]	[0.001, 1.0]	Uniform
	(31) Maximum shear stress of penetration tube multiplier [-]*	[0.1, 10.0]	Uniform

(*) Parameters introduced as a result of code revisions to the MAAP5 code

Following the methodology of Rahman et al. [3], the core damage time and reactor vessel failure time were used to evaluate the core damage frequency and RV failure frequency after correcting for a 10-

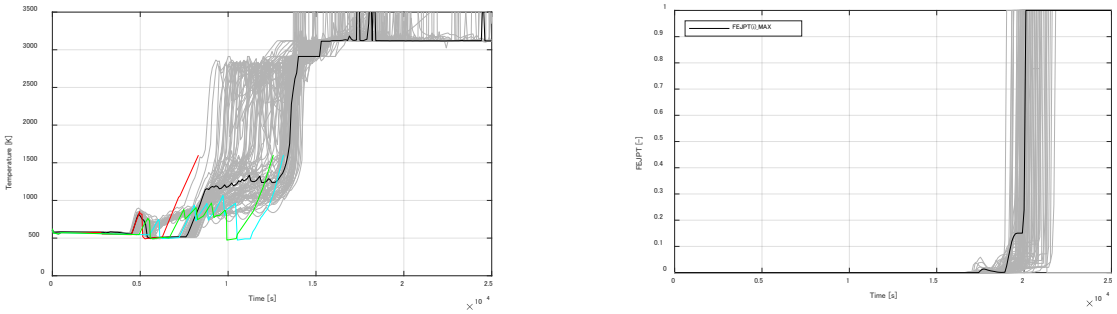

(a) Rod surface temperature (b) Penetration tube ejection parameter

Figure 3: Uncertainty analysis results

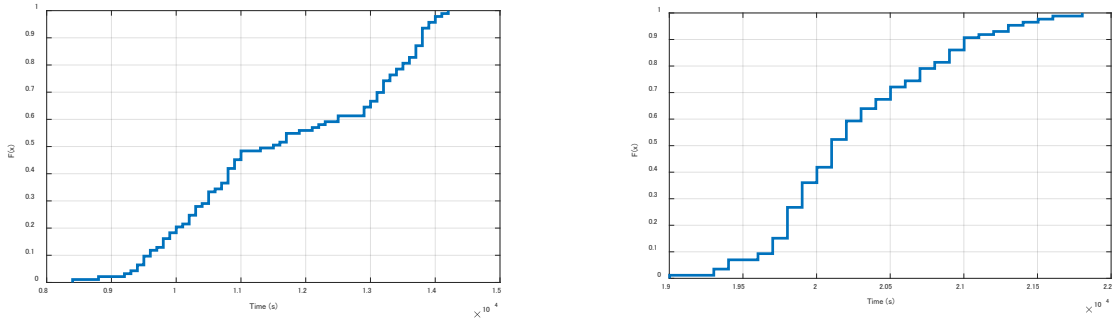

(a) Core damage timing (b) Reactor vessel failure timing

Figure 4: Core damage and reactor vessel failure timings

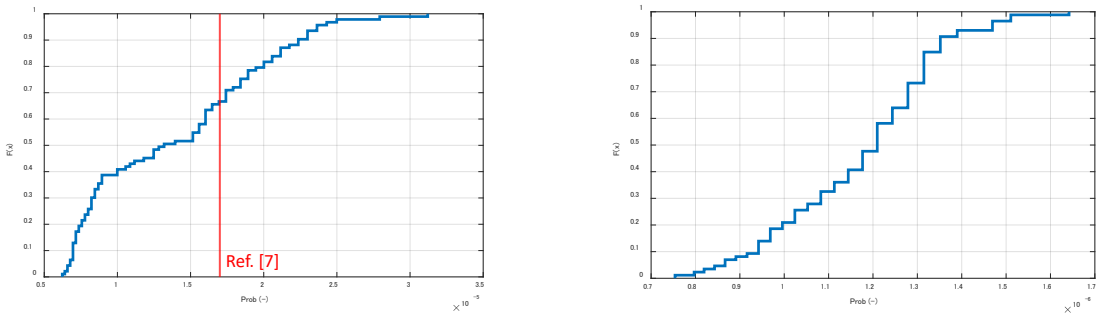

(a) Core damage probability (b) Reactor vessel failure probability

Figure 5: Core damage and reactor vessel failure probabilities

minute delay (based on [8]) relative to the latest SI initiation time. Specifically, the core damage frequency and RV failure frequency for each case of the accident sequence were calculated by multiplying the initiating event frequency of the loss of offsite power by the failure probabilities of the emergency power system, auxiliary feedwater system, and pump seal failure, and then correcting as follows:

$$CDF(i) = P_{IE-LOSP} \times P_{EPS} \times P_{L1-SBO} \times (1 - P_{SL-S}) \times P_{FPR}\left(t_i^{CD} - 10min\right) \quad (2)$$

$$VBF(i) = P_{IE-LOSP} \times P_{EPS} \times P_{L1-SBO} \times (1 - P_{SL-S}) \times P_{FPR}\left(t_i^{VB} - 10min\right) \quad (3)$$

Fig. 5(a) shows the cumulative distribution function (CDF) of the core damage probability. The core damage probability ranged from 6.23E-6 to 3.12E-5. The median was 1.32E-5, and that was close to

the estimated value of 1.7E-5 in the PSA reports [6-7]. Fig. 5(b) shows the CDF of the RV failure probability. The reactor vessel failure probability ranged from 7.54E-7 to 1.64E-6. The median was 1.21E-6.

4.3. Contribution of the Uncertainty Parameters

To quantify the contribution of epistemic uncertainty in MAAP5 model parameters to severe accident progression, a parameter importance analysis was performed using SHAP (SHapley Additive exPlanations) values. This analysis focused on FEJPT, a failure indicator representing RV failure due to penetration tube ejection. The base-10 logarithm of the FEJPT parameter calculated by MAAP5, $\log_{10}$(FEJPT), was used as the target variable for the analysis. Fig. 6 shows the CDF of $\log_{10}$(FEJPT).

A surrogate model was constructed using a random forest regressor to map the relationship between the uncertainty parameters and the FEJPT output, and SHAP values were computed to quantify the contribution of each input parameter to the variation in FEJPT. A SHAP summary plot was generated to visualize both the magnitude and direction of these parameter contributions, as shown in Fig. 7. In this plot, each point represents a simulation sample; the horizontal axis corresponds to the SHAP value (i.e., the contribution to the FEJPT output), and the color indicates the relative magnitude of the parameter value. This representation allows for the simultaneous assessment of parameter importance and correlation structure.

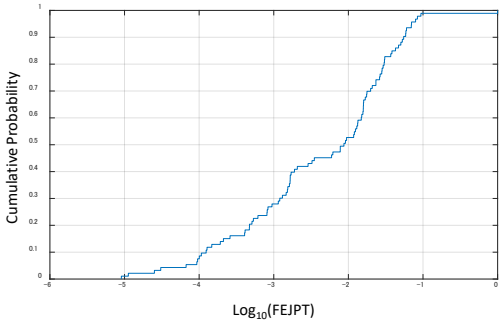

Figure 6: CDF of $\log_{10}$(FEJPT)

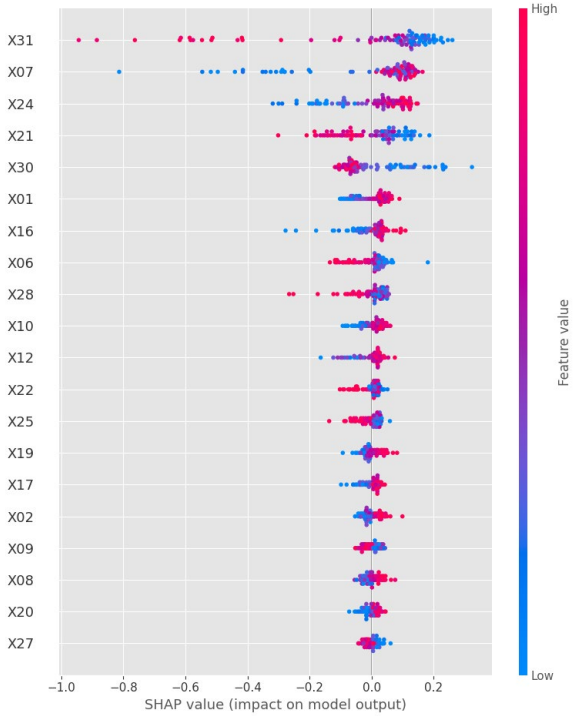

Figure 7: SHAP summary plot

The analysis identified parameters with dominant contributions to the variability of FEJPT. Specifically, parameters associated with penetration tube strength, heat transfer characteristics, and lower head thermal-hydraulic behavior exhibited a strong influence on the progression toward RV failure. Furthermore, the SHAP summary plot revealed non-linear and non-monotonic relationships between input parameters and FEJPT. These results provide insights into which epistemic uncertainties most significantly affect reactor vessel failure risk. Such information is valuable for prioritizing model improvement efforts and for enhancing the transparency of uncertainty propagation in dynamic event tree–based risk assessments.

5. CONCLUSION

This study investigated the contribution of epistemic uncertainties in MAAP5 physical model parameters to severe accident progression and risk metrics using a DET framework for a SBO scenario.

Thirty-one uncertainty parameters associated with key physical phenomena in the TMLB' scenario were identified based on PIRT analyses and related literature. The 93 MAAP5 simulations were performed to evaluate the variability in core damage timing, RV failure timing, and associated risk

metrics. The results showed that while core damage timing exhibited a bimodal distribution due to uncertainties in thermal-hydraulic processes such as condensation during accumulator injection, RV failure timing followed a unimodal distribution. The estimated core damage probability and RV failure probability were found to be consistent with previously reported PSA results.

To further interpret the impact of uncertainty parameters on severe accident progression, a SHAP-based contribution analysis was performed using a surrogate model. The analysis identified several dominant parameters affecting the RV failure indicator (FEJPT), including those related to penetration tube strength, heat transfer characteristics, and lower head thermal-hydraulic behavior. In addition, the SHAP summary plot revealed non-linear and non-monotonic relationships between input parameters and the RV failure indicator, indicating complex interactions among accident progression phenomena.

The results demonstrate that the integration of DET simulations with explainable machine learning techniques provides a useful framework for identifying influential epistemic uncertainties in severe accident analysis. Such information can support prioritization of model improvement efforts and enhance the interpretability of uncertainty propagation in dynamic PRA.

Future work will focus on extending the proposed approach to larger parameter sets and more complex accident scenarios, as well as investigating its applicability to full dynamic PRA frameworks, including the treatment of both epistemic and aleatory uncertainties in an integrated manner. This framework also provides a basis for more systematic and structured representations of uncertainty propagation in complex risk models.

References

[1] N. Siu, “Risk Assessment for Dynamic Systems: An Overview”, *Reliability Engineering and System Safety*, **43**, pp.43-73 (1994).

[2] P. E. Labeau, C. Smidts, S. Swaminathan, “Dynamic Reliability: Towards an Integrated Platform for Probabilistic Risk Assessment”, *Reliability Engineering and System Safety*, **68**, pp.219-254 (2000).

[3] S. Rahman, D. R. Karanki, A. Epiney, O. Zerkak and V. N. Dang, “Ranking of Uncertain Parameters for Dynamic Event Tree Analysis: A Case Study Based on a Station Blackout Scenario”, NURETH-16, Chicago, IL, August 30-September 4 (2015).

[4] Electric Power Research Institute, "MAAP5 Modular Accident Analysis Program for LWR Power Plants User's Manual", EPRI, Palo Alto, CA: (2011).

[5] S. M. Lundberg, and S.-I. Lee, “A Unified Approach to Interpreting Model Predictions”, Advances in Neural Information Processing Systems, NeurIPS (2017).

[6] M. B. Sattison, K. W. Hall, “Analysis of core damage frequency: Zion, unit 1 internal events”, US NRC, NUREG/CR-4550, EGG-2554, Vol. 7, Rev. 1. (1990).

[7] Safety Margin Assessment and Application – Final Report, NEA/CSNI/R(2011)3, Committee on the Safety of Nuclear Installations (CSNI), Nuclear Energy Agency, Paris, France (2011).

[8] F. Fouet, P. Probst, J.M. Lanore, “Application of SMAP Methodology to a 10% power up-rate for Zion NPP SBO Transient”, PHYSOR – Advances in Reactor Physics to Power the Nuclear Renaissance, Pittsburgh, Pennsylvania, USA, May 9-14 (2010).

[9] Atomic Energy Society of Japan, “Report on Investigation of Severe Accident Evaluation”, Severe Accident Evaluation Research Committee (2014) (in Japanese).

[10] Japanese PWR Utilities, “Severe Accident Analysis Codes for Evaluating the Effectiveness of Accident Management Measures (Part 3: MAAP)”, (in Japanese).

[11] S.S. Wilks, “Statistical Prediction with Special Reference to the Problem of Tolerance Limit,” *Annals of Mathematical Statistics*, **13**, pp.400-409, (1942).